Int J Adv Manuf Technol (2018) 94:1981–1989
DOI 10.1007/s00170-017-0966-x

ORIGINAL ARTICLE

Research on the ductile-mode machining of monocrystalline silicon using polycrystalline diamond (PCD) tools

Jinxuan Bai[1] · **Qingshun Bai**[1] · **Chao Hu**[1] · **Xin He**[1] · **Xudong Pei**[1]

Received: 30 March 2017 / Accepted: 14 August 2017 / Published online: 2 September 2017

Abstract This article presents an experimental investigation on high-efficiency machining monocrystalline silicon by polycrystalline diamond (PCD) end mills with a tool diameter of 5 mm. The milling experiments were carried out on a self-made five-axis numerical control machine tool. A super-high magnification zoom lens 3D microscope, white light interferometer, and dynamometer were applied to qualitatively and quantitatively characterize the performance of processed surfaces and cutting force. A surface roughness of Ra = 9.9 nm, better than most previously reported value on silicon, was obtained. Also, greater plastic removal efficiency was achieved under a small axial depth of cut and feed rate (less than 60 and 0.3 μm/tooth, respectively) and high spindle speeds (50,000 rpm). Moreover, surface characterization studies were explored which reveals that faster spindle speed, lower feed rate, and smaller cut depth can provide an easy access to ductile machining. At last, note that the shape structure and amplitude of cross-cutting force kept a close relation with the processing mode of single-crystal silicon, and a stable cross force contributed to improve surface quality as well as inhibiting micro-crack initiation.

Keywords High-efficiency machining · Ductile cutting · Monocrystalline silicon · Surface topography · Surface roughness

✉ Qingshun Bai
qshbai@hit.edu.cn

[1] School of Mechanical and Electrical Engineering, Harbin Institute of Technology, Harbin 150001, China

1 Introduction

Currently, hard brittle materials such as single-crystalline silicon and germanium are successfully applied in infrared optical lenses, micro-electro-mechanical systems (MEMS), and precise mechanic industrial sectors [1, 2]. Fabrication of high-accuracy monocrystalline silicon miniature components with dimensions from microns to millimeters is a developing tendency. However, due to low relative machining accuracy and poor surface finish, traditional etching technology is inadequate to process micro-devices and components. In addition, although focus ion beam (FIB) and femtosecond laser methods have shown some advantages in micro-processing, the problems of inefficiency, high cost, and small processing range impeded their wide industrial application [3, 4]. To overcome the above constraints, improvement on traditional machining process and development of substitution machining technologies are being investigated.

Single-point diamond cutting technology is a typical precision processing method, which has been applied in fabricating the free from surface of components with excellent machining quality over different engineering materials, such as processing copper [5], inconel alloy [6], and stainless steel [7]. Although silicon is brittle, it has intensive dislocation activity in specific environment [8, 9]. For a better understanding of plastic deformation mechanism in the material removal process of monocrystalline silicon, the nanometric deformation behavior in defect-free single-crystal silicon was demonstrated by molecular dynamics technology [10]. Results showed that a critical criterion can be adopted to determine whether plastic deformation or micro-crack initiation would dominantly take place. If the plastic deformation behavior is prior, ductile removal mode will be achieved. Subsequently, this principle was widely used in ductile cutting brittle materials and crystals, such as silicon [11], germanium [12], silicon carbide [13] and glass [14]. Fang et al. [15] presented an investigation on

diamond turning of monocrystalline silicon to elucidate the microscopic origin of ductile-regime machining. Result showed that ductile removal is principal if the uncut chip thickness reaches the threshold of ductile cutting. Liu et al. [16] reported the experimental results of machining silicon carbide ceramics and suggested that grinding can increase plastic deformation ability of workpiece in contact zone as well as improve finished surface performance. Especially, compared with the above cutting methods, milling technology is expected to have more enormous potential to cost effectively fabricate 3D products with high accuracy and good surface finish [17].

Conventionally, small radius end mills with high form precision were used to plastic milling monocrystalline silicon device. In previous literatures, in order to obtain a crack-free surface, the tool diameter was always set to 0.5 mm [18] or even smaller [19]. Huo et al. adopted the diamond-coated fine-grain tungsten carbide mills with a tool diameter of 0.5 mm to study the formative mechanism of surface and subsurface during micro-milling monocrystalline silicon process [17]. Also, the feed per tooth is just a few nanometers and the axial depth of cut is usually less than 0.5 μm in past studies [19, 20]. Rusnaldy et al. presented micro-end milling of monocrystalline silicon experimental investigation with extreme small cutting parameters (axial cut depth and feed rate are less than 0.3 and 0.0012 μm/tooth, respectively) to study the interactive relation between cutting force and surface quality [20]. As a result, although a good surface finish can be obtained, the process is inefficiently with a low brittle material removal rate. In fact, during micro-milling process, some issues such as intermittent cutting process, transient impact loads, and continuous changing uncut chip thickness make machining process much more complex compared with turning and grinding methods.

In this work, we attempted to conduct the experimental investigation of ductile milling single crystal silicon to solve the inefficiency of machining mentioned above. This study aims at achieving equivalence both in high production efficiency and good machined surface quality. Organization for this paper is as follows. Initially, Section 2 introduces the micro-milling setup and measurement instruments. Then, Section 3 analyzes and discusses the experimental results, such as surface topography, surface roughness and cutting force. At last, the manuscript is concluded with some final remarks.

2 Experimental methodology for micro-milling monocrystalline

2.1 Experimental setup

A self-made five-axis milling numerical control machine tool was employed to process monocrystalline silicon micro-slots as shown in Fig. 1. The dimensions of machine tool are 580 mm × 500 mm × 770 mm. In this instrument, *X* axis, *Y* axis, and *Z* axis are straight-line axes, and the *B* axis and *C* axis are rotational axes. A CCD camera was mounted to align micro-tools and monitor the machining process. A dynamometer was installed beneath the workpiece holder to record the cutting force in the milling process. In addition, the maximum speed of air-bearing spindle can reach 8×10^4 rpm, and the runout is less than 1 μm. The straightness positional precision of that machine tool can achieve ± 0.35 μm/10 mm. The (1 1 1) single-crystal silicon samples were bonded to a ground metal plate. The diameter and thickness of silicon samples are 35 and 4 mm, respectively. The perpendicularity between tool and silicon sample surface was repeatedly confirmed to ensure a uniform axial depth of cut.

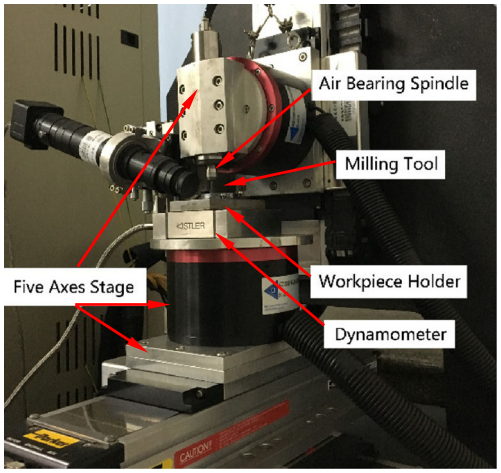

Fig. 1 The experimental facility for milling along [1–1 0] direction on a (111) monocrystalline silicon samples

2.2 Experimental tools

Figure 2a, b shows the brand-new polycrystalline diamond (PCD) micro-end mills used in the present research work. The PCD tools have a nominal tool diameter of 5 mm, cutting edge radius of 40 μm, and nominal rank angle of −2°. The edge radii were measured on Dino-Lite AM413T5 electron

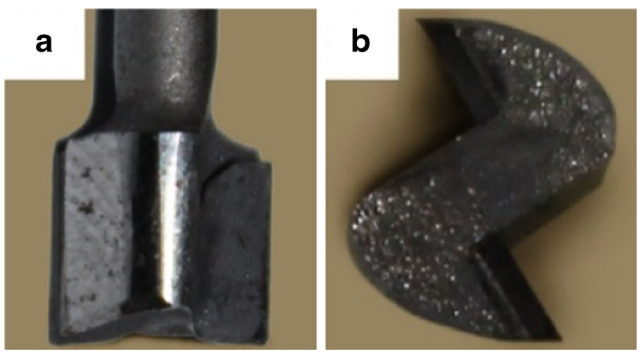

Fig. 2 Images of tool. **a** Optical photography of micro-end mill. **b** Optical photography of cutting edge

microscope by fitting a circle. During micro-machining brittle materials, the edge radius is directly tied to the critical value of uncut chip thickness, h_c, which is one of the important parameters to achieve ductile processing. It can be calculated by $h_c = R_e(1 + \sin\alpha)$, R_e is the edge radius and α is nominal rake angle. In addition, compared with diamond coated tools, the interior particles of PCD mills have equal strength and toughness which contributes to limiting the flank face breakage of micro-tool caused by intermittent impact load.

2.3 Experimental preparation

All tests were immersion slot milling in the present study. For each experiment, a 20-mm-long and 5-mm-wide micro-slot was processed. The feed direction was conducted along [1–1 0]. In order to avoid contamination, the processing method was dry machining. Three controllable variables were performed, such as axial depth of cut (μm), feed rate (μm/tooth), and spindle speed (rpm). To fully disclose all of the main influence factors and their interaction, the 4 × 4 × 3 mixed-level full cutting conditions were conducted, as shown in Table 1. In this matrix, four levers of cut depth, four levers of feed rate, and three levers of spindle speed were selected, which can make a more comprehensive evolution than existing literatures [18–20]. In order to eliminate the influence of tool wear on machined surface precision and edge chipping, three micro-end mills with equal accuracy were used for the experiments. During micro-machining process, a total of 12 slots were divided into three groups in order and hence milled by each cutter.

2.4 Experimental measurement

During micro-milling process, the cutting force was measured by 9250C2 dynamometer made by Kistler, which was directly fixed on the worktable. After milling, the finished slot surfaces were cleaned by the ultrasonic bath. To reveal whether the micro-slots were in plastic removal or not, the surface topography of micro-slots was carefully detected under a VHX-1000E super-high magnification zoom lens 3D microscope made by Keyence. Meanwhile, the surface roughness of machined surface was measured by Talysurf CCI 2000 white light interferometer. For micro-slots, the surface finish values of different positions were detected in the transverse direction, and then the average values were calculated.

3 Results and discussions

Both qualitative and quantitative analyses were implemented to characterize the surface quality and obtain the evolution rule of cutting force profile during micro-machining monocrystalline silicon slots. A distinct cutting parameter dependence behavior can be observed. The experimental results and measurement techniques were discussed in this section.

3.1 Surface topography of machined monocrystalline silicon slot surface

A large number of cutting conditions were explored to obtain the best finished surface. After processing, the bottom surfaces of

Table 1 Experimental matrix of micro-machining of monocrystalline silicon and responses: measured surface roughness, cutting force mode and cutting mode

Test no.	Axial depth of cut (μm)	Feed rate (μm/tooth)	Spindle speed (rpm)	Surface roughness[a] Ra (μm)	Cutting force[b] (S/PS/C)	Cutting mode[c] (D/PD/B)
1	10	0.075	50,000	0.009	S	D
2	30	0.075	50,000	0.010	S	D
3	60	0.075	50,000	0.014	S	D
4	120	0.075	50,000	0.145	C	B
5	30	0.15	50,000	0.010	S	D
6	30	0.3	50,000	0.016	S	D
7	30	0.6	50,000	0.021	PS	PD
8	60	0.15	50,000	0.016	S	D
9	60	0.3	50,000	0.077	PS	PD
10	60	0.6	50,000	0.106	C	B
11	10	0.075	40,000	0.079	PS	PD
12	10	0.075	20,000	0.129	C	B

[a] Surface roughness values presented in the above table are the mathematic average for measured Ra

[b] *S*—smooth mode; *PS*—partial smooth mode; *C*—chaos mode

[c] *D*—ductile mode; *PD*—partial ductile mode; *B*—brittle mode

monocrystalline silicon micro-slots were detected by ultra-depth microscope. The microscopic images were shown in Fig. 3 (pictures (a) ~ (i) directly correspond to the test no. 1 ~ 12). It is clear that the multiple types of surface defects can be found on the machined surface, such as micro-debris, micro-crack, and irregular streak. In this study, the shape and distribution of defects were adopted to determine the machining mode. In Fig. 3a–c, e, f, h, milled surfaces are ultra-smooth without obvious defects or machining marks, which indicate that the ductile mode machining was achieved. Specially, a few scattered flaws as well as tiny pits or cracks remained on slot surfaces (as Fig. 3g, i, k), which shows an intermediate (partial ductile) milling mode happened in those cutting conditions. The partial ductile removal process results in a semi-smooth surface structure. In addition, lots of brittle damages and disorder cutting marks within fractures and fragments (as shown in Fig. 3d, j, l) left on processed surfaces can be regarded as brittle machining.

In order to further reveal the generation mechanism of surface defects to explore preventive measures, selected local detail images of slot surface and corresponding 3D topography under various milling modes are shown in Fig. 4. Under ductile mode, the milling paths are stabilized and cleared on the bottom of slot surfaces, and there is no micro-crack, tearing, or chipping (as shown in Fig. 4 (a) and (b)). Meanwhile, the 3D topographic features indicated that the ductile milling mode can greatly suppress and control the formation of surface defects. Moreover, although partial ductile mode would occasionally produce irreversible damages, the plastic removal is still an initiative process, and only bits of burrs and micro-damages can be found in local region (as Fig. 4 (c)). Therefore, a good processed surface topography also can be achieved. Figure 4 (d) showed that brittle cutting method always brings apparent waviness of processing paths in slot surface, which is considered as a warning sign of destruction chipping. Besides, the 3D topographic feature suggested that brittle finished surface is full of rugged and chaotic burrs, which would greatly affect the geometric accuracy and induce potential surface functional failure of machined components.

The experimental results indicated that feed rate, axial depth of cut, and spindle speed play an important role in generating a high-accuracy surface. The cutting modes of all tests were shown in Table 1. In this study, the ductile milling mode can be obtained at a

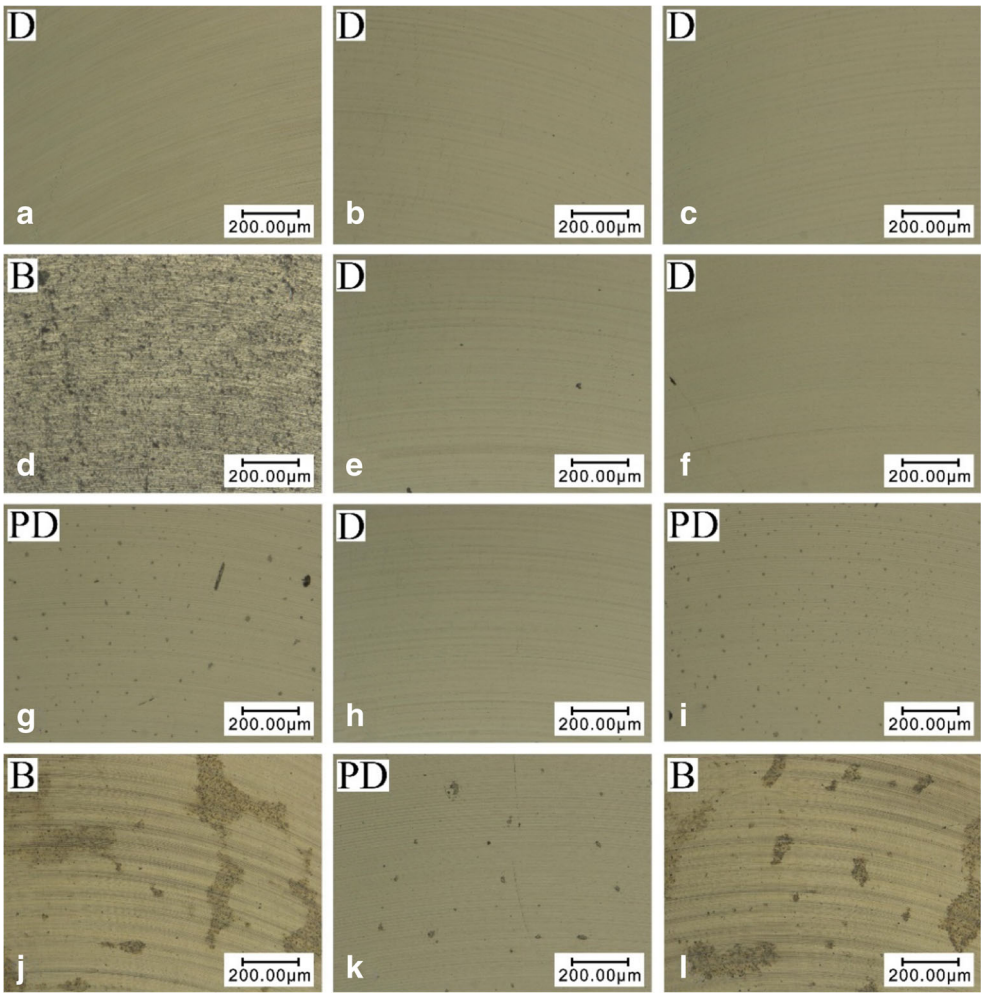

Fig. 3 Finished surface topography at various different axial depths of cut, feed rates, and spindle speeds. *D* ductile mode, *PD* partial ductile mode, *B* brittle mode

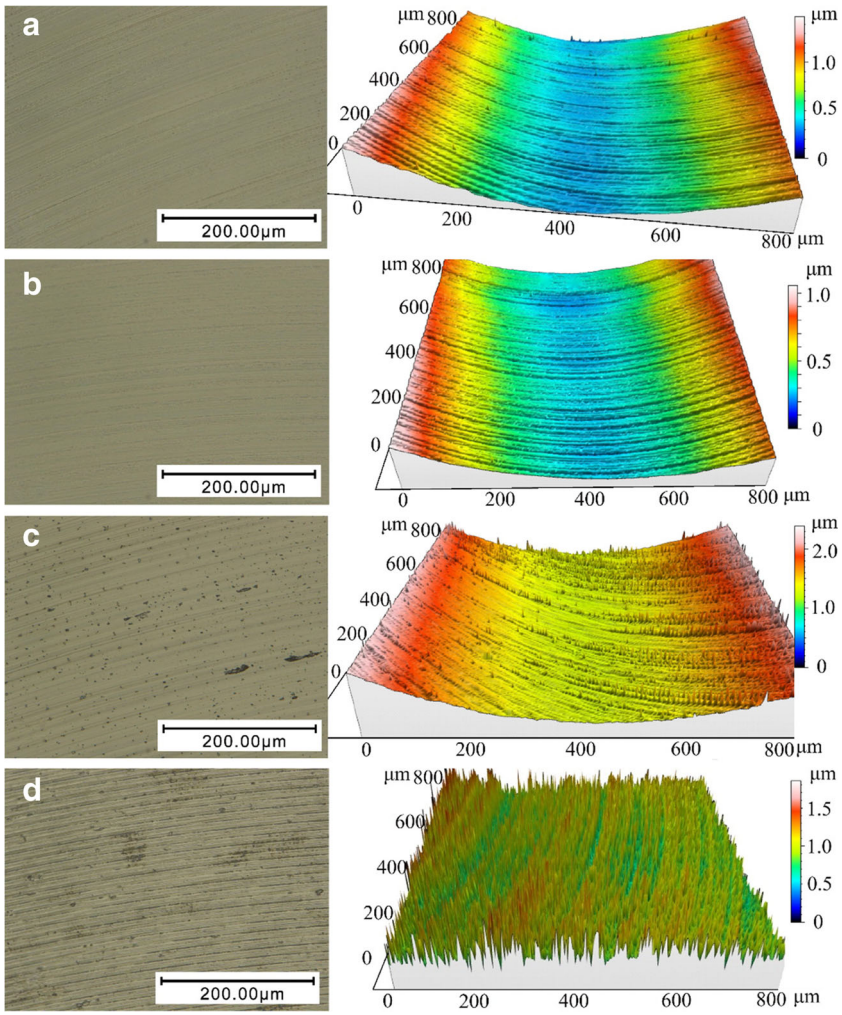

Fig. 4 Selected cutting surface local detail images and corresponding 3D topography. (a)—Test no. 3; (b)—test no. 6; (c)—test no. 7; (d)—test no. 10

small axial depth of cut and feed rate (less than 60 and 0.3 μm/tooth, respectively) and high spindle speeds (50,000 rpm). It can be seen that the smaller feed rate and cut depth can facilitate fewer surface damages and hence boost ductile mode processing. In addition, under the same cut depth and feed rate, the relatively high spindle speed makes cutting process more easy to achieve ductile removal. This is because a larger spindle speed can increase cutting speed and decrease the uncut cutting thickness. Moreover, in micro-machining of monocrystalline silicon, large axial depth of cut has a negative effect on performed surface. Under the depth cut being 120 μm, the machined surface has the largest surface damage region and worst cutting quality, as shown in Fig. 3d.

3.2 Influence of processing parameters on machined surface quality

To further quantitatively investigate the inner influence of various cutting parameters to slot surface characteristic and obtain their optimal combination, the arithmetic surface roughness, Ra, which can acquire the information of average surface geometry, was adopted to reveal the effect on surface formation. The surface roughness of the micro-slots was measured by a Talysurf CCI 2000 white light interferometer. For every micro-slot, three random positions along cross sections were detected and the mathematic average values were calculated in Table 1. In addition, all of initial data was shown in Table 2 (Appendix).

The results of experiment indicated that ultra-precision level surface finish has been achieved within the range of cutting parameters. Especially, the surface roughness measured is much better than the other existing studies [17–20] under ductile and partial ductile mode. Among them, the surface roughness value, 0.009 μm, has been far less than the prior optimal result, 0.039 μm [17]. The improvement of surface finish value reaches up to 76.9%. In addition, it is worth mentioning that the nominal diameter of the mill used in this study is about ten times larger than conventional ones. Not only the tool but also the feed rate and axial depth of cut both jumped over the parameter scope of traditional processing. Hence, the present research has achieved better surface performance as well as greater removal efficiency, which rises no less than 20 times. To further reveal the influence of every cutting parameter on surface precision, the evolution law of surface roughness was plotted in Fig. 5.

As shown in Fig. 5a, the invariable milling parameters were configured: 0.075 μm/tooth for feed rate and 50,000 rpm for spindle speed. Meanwhile, the axial depth of cut changed from 10 to 120 μm. The curve suggested that cut depth has tremendous and negative impact to surface roughness, i.e., the ever-increasing level of cut depth degenerates slot surface quality. The ductile cutting mode has been achieved when the cut depth is less than 60 μm. When the axial depth of cut is from 10 to 60 μm, there is only a 4.37-nm increase in slot surface finish value. Yet once the axial depth of cut increases from 60 to 120 μm, a nearly 936% increase in roughness average value can be observed. The reason is that the mills have produced cutting edge radius size effect when the undeformed chip thickness is small enough. Actually, monocrystalline silicon can be ductility machined, yielding plastic chips under the influence of sufficient compressive stress. According to dislocation theory, the magnitude of deviatoric has decided the yield strength of brittle materials, while its stress state determines the ductile-brittle transition behavior of a fracture. Therefore, larger negative rake angle tools were widely used to generate the necessary hydrostatic stress into contact zones during the micromachining silicon process. This results in the monocrystalline silicon in front of cutting edge bearing adequate vertical pressure. However, because of complicated construction and small dimension of micro-end mills, commercial tools were difficult to be fabricated with enough large negative rake angle. Particularly, the micro-end mills could form effective negative rake angle if undeformed chip thickness is at the same level as the edge radius, which is called as size effect, as shown:

$$\alpha_e = \arcsin\left(\frac{h}{R_e} - 1\right) \quad \text{for} \quad h < h_c \tag{1}$$

$$\alpha_e = \alpha \quad \text{for} \quad h > h_c \tag{2}$$

where α_e is effective rake angle, α is nominal rake angle, h is undeformed chip thickness. Therefore, an appropriate selection of undeformed chip thickness has contributed to ductile mode removal of silicon and improved cutting efficient. But once the stable process is broken by inappropriate cutting parameters or irregularity machine tool vibration, the cutting force will fluctuate in vertical axial, which may cause the failure of plastic removal and degrade the integrity of finished surface. The supposition has been studied in more detail later in this article.

As shown in Fig. 5b, the spindle speed changed from 20,000 to 50,000 rpm, while the remaining arguments kept exactly the same (feed speed 0.075 μm/tooth and axial depth of cut 10 μm). The experimental results showed that there is a maximum 89.1% decline in surface roughness value with the increasing of spindle speed, and ductile machining can be achieved under the spindle speed of 50,000 rpm. This suggested that higher spindle speed not only achieves higher removal rate but realizes better surface finish. Figure 5c demonstrated how the slot surface roughness varies when the feed rate changes. The morphologies of two slot surfaces which were separately processed under the cut depths of 30 and 60 μm are presented. As expected, the surface finish is apt to deteriorate with the increase of feedrate. When the feed rate is less than 0.15 μm/tooth, the plastic removal is dominant. As the feedrate increases from 0.3 to 0.6 μm/tooth, there is around

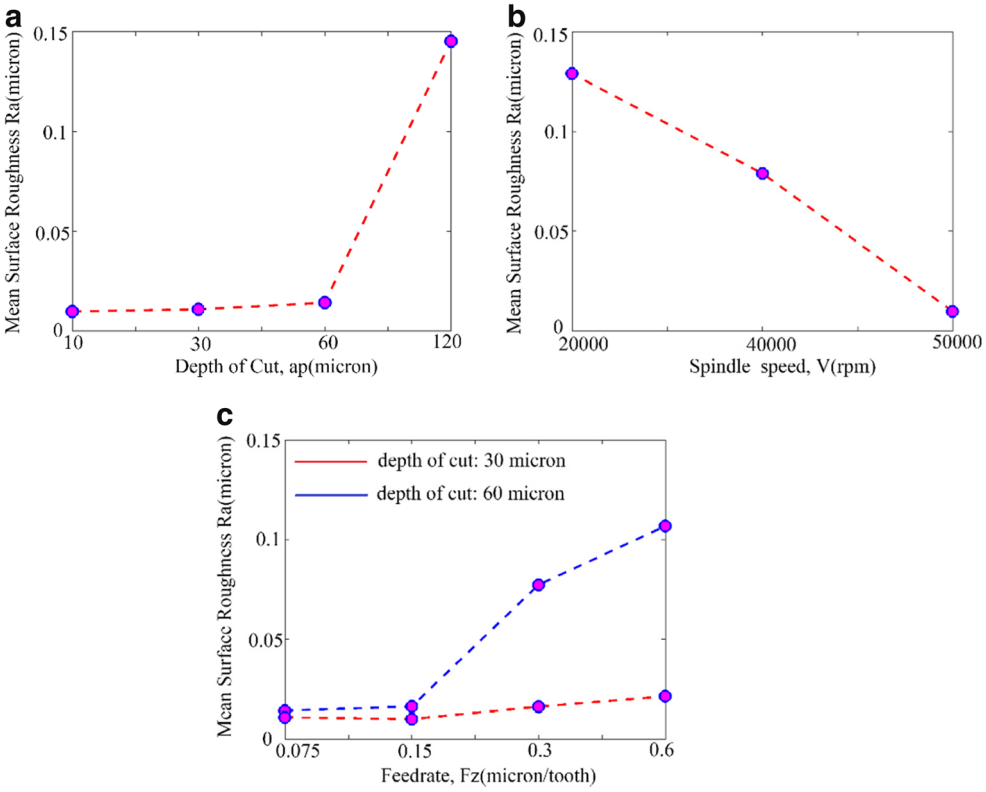

Fig. 5 The influence plots of single factor on surface roughness. **a** Depth of cut. **b** Spindle speed. **c** Feed rate

562.5% increase in surface roughness value under 60 μm for axial depth of cut, while only 110% increase in surface finish value under 30 μm for axial depth of cut. The above results indicated that the interaction between feed rate and axial depth of cut also have influence on the surface precision. Therefore, an appropriate combination of cutting parameters is not negligible. In this work, the optimal parameters assembly is that axial depth of cut (10 μm), feed rate(0.075 μm/tooth), and spindle speeds (50,000 rpm).

3.3 Cutting force evolution mechanism during micro-milling monocrystalline silicon process

When machining monocrystalline silicon with small-diameter tools, feed force is dominant and the broad crater wear on rake face is serious. But once the large radius tools were used, the cutting force in thrust direction, cross force, becomes paramount and the injury pattern is mainly caused by the formation of angular flank wear. The reason is that, for large radius end mills, the effective rake angle is usually negative when the undeformed chip thickness is less than the cutting-edge radius. The negative rake angle can reduce stress concentration and produce a relatively uniform cutting stress field, which is similar to the hydrostatic stress filed. Hence, the cross-force component is dominant. However, if the boundary of stability cutting conditions was broke down, the cross force would be intermittent and disorganized. Specially, the present experimental results showed that the shape-structure and amplitude of cross force were patently germane to surface topography and surface accuracy.

Selected measured cross-force signals in time domain were shown in Fig. 6. The cross force in certain time domain was obtained by Kistler 9250C2 dynamometer, which have various profiles under different cutting conditions. Like evaluating material removal mode, the regularity and stability of cross-force profiles were adopted to elucidate cutting force mode. Figure 6a was the cross-force profile under 10 μm for cut depth, 0.075 μm/tooth for feed rate, and 50,000 rpm for spindle speed. It can be seen that the amplitude of cross force almost keeps stable, and the profile is smooth and constant without dithering or halts. Note that the corresponding processed surface achieved in fracture-free performance as well (example is shown in Fig. 3a). Likewise, few local vibrations and burrs interference on cross force indicated that the partial smooth cutting force profile has taken place (example is shown in Figs. 6b, and 3i suggested that machined surface is intermediate ductile removal machining accordingly. Specially, the cross-force signal of Fig. 6c is chaotic and intermittent. The cutting traces are blurred, and there are massive micro-cracks and chippings on the slot surface, as shown in Fig. 3d. Further, the rest of the analysis results were carried out in Table 1.

According to the above researches, smooth cross-force profile is benefited to inhibit surface micro-damages and improve machining quality. Instead, partially smooth and chaotic mode of cross-force profiles can degenerate the processing effectiveness. This is mainly because that the transient distortion of cross force signal tends to form high frequency and irregular transient impact stress into slot surface. For monocrystalline silicon, the impact effect would disturb the intrinsic dislocation evolution process and induce persistent dislocation slip bands in silicon slot surface, which can result in stress concentration and heterogeneous deformation in the interior of the grains. Ultimately, the abovedescribed behavior will significantly decrease slot surface roughness value and induce the micro-crack initiation.

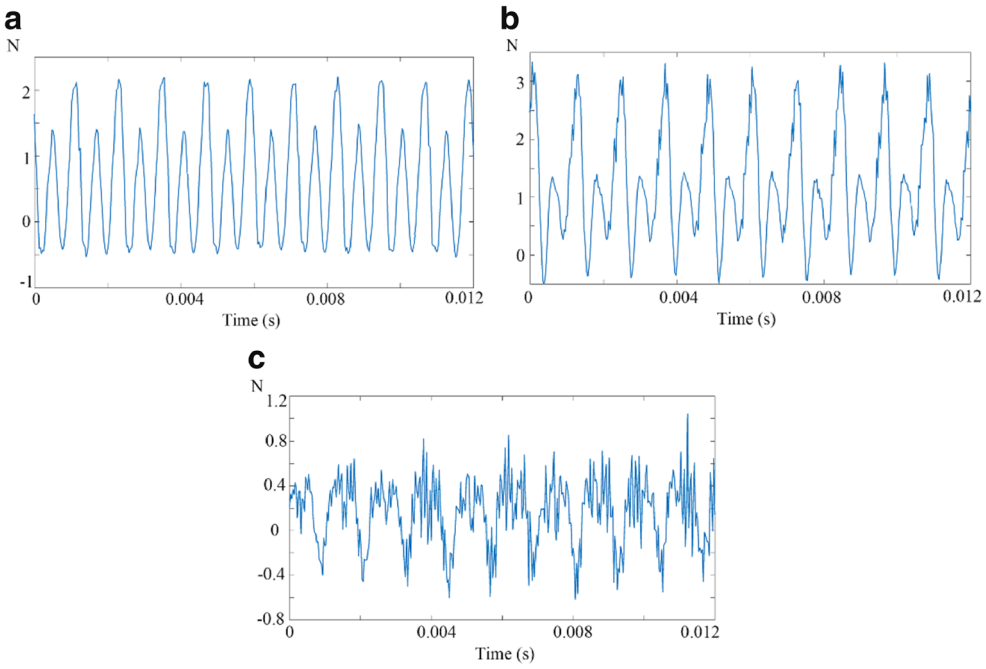

Fig. 6 Selected measured cross feed force during micro-milling process. **a** Test no. 1. **b** Test no. 9. **c** Test no. 4

4 Conclusion

High-efficiency milling monocrystalline silicon experiments were performed with polycrystalline diamond (PCD) tools. Fundamental characteristics of the machining process, such as surface topography, roughness, and cutting force, were detected. The following results can be concluded from this work:

1. Influence of machining parameters on micro-milling of monocrystalline silicon was obtained by surface topography analysis. The experimental results suggested that feed rate, axial depth of cut and spindle speed have significant effects on surface formation. The ductile removal mode can be achieved under a small axial depth of cut and feed rate (less than 60 and 0.6 μm/tooth, respectively) and high spindle speeds (50,000 rpm).
2. Mean surface roughness of 9.9 nm on the slot surface of monocrystalline silicon can be obtained during ductile cutting process. The improvement of surface finish value reaches up to 76.9% compared with prior optimum under the same condition. Meanwhile, the optimal machining parameters can be gained as follows: axial depth of cut (10 μm), feed rate (0.075 μm/tooth), and spindle speeds (50,000 rpm).
3. In the present study, the augmented diameter of micro-end mill and increased machining parameters range not only achieve good surface quality but promote greater removal efficiency, which goes up at least 20 times than traditional process.
4. Results showed that the shape structure and amplitude of cross force is intimately related to machined surface topography and surface finish during micro-machining monocrystalline silicon process. Continuous and stable cross force can enhance ductile mode machining.

Acknowledgements This research work was jointly supported by the National Natural Science Foundation of China (Grant No. 51575138) and the State Key Program of National Natural Science Foundation of China (Grant No. 51535003).

Appendix
Initial measured results

Table 2 Machined surface roughness results at different conditions

Responses	Surface roughness Ra (nm)											
Exp. no.	1	2	3	4	5	6	7	8	9	10	11	12
Test.1	11.856	9.360	18.161	147.162	9.807	14.677	23.943	17.759	53.166	111.68	81.820	155.806
Test.2	9.292	12.835	13.352	127.724	10.131	19.671	15.984	15.707	89.999	108.877	60.010	122.468
Test.3	8.612	10.725	11.369	161.019	10.396	15.139	24.358	15.650	89.216	99.913	86.318	108.85

References

1. Du J, Wen HK, Young DJ (2004) Single crystal silicon MEMS fabrication based on smart-cut technique. Sensor Actuat A-Phys 112(1):116–121
2. Wu YQ, Huang H, Zou J (2013) A focused review on nanoscratching-induced deformation of monocrystalline silicon. Int J Surf Sci Eng 7(1):51–80
3. Kalhor N, Boden SA, Mizuta H (2014) Sub-10 nm patterning by focused He-ion beam milling for fabrication of downscaled graphene nano devices. Microelectron Eng 114(114):70–77
4. Danilovab PA, Zayarnyia DA, Ionina AA, Kudryashovab SI, Makarova SV, Rudenko AA, Yurovskikh VI, Kulchin YN, Vitrik OB, Kuchmizhak AA, Drozdova EA, Odinokov SB (2014) Mechanisms of formation of sub- and micrometre-scale holes in thin metal films by single nano- and femtosecond laser pulses. Quantum Electron 44(6):540–546
5. Filiz S, Conley CM, Wasserman MB, Ozdoganlar OB (2007) An experimental investigation of micro-machinability of copper 101 using tungsten carbide micro-endmills. Int J Mach Tools Manuf 47(7–8):1088–1100
6. Lu XH, Jia ZY, Wang H, Si LK, Liu YY, Wu WY (2016) Tool wear appearance and failure mechanism of coated carbide tools in micro-milling of Inconel 718 super alloy. Ind Lubr Tribol 68(2): 267–277
7. Coppel R, Abellan-Nebot JV, Siller HR, Rodriguez CA, Guedea F (2016) Adaptive control optimization in micro-milling of hardened steels-evaluation of optimization approaches. Int J Adv Manuf Tech 84(9):2219–2238
8. Korte S, Barnard JS, Stearn RJ (2011) Deformation of silicon—insights from microcompression testing at 25–500°C. Int J Plasticity 27(11):1853–1866
9. Cai W, Bulatov VV, Justo JF (2000) Intrinsic mobility of a dissociated dislocation in silicon. Phys Rev Lett 84(15):3346–3349
10. Tanaka H, Shimada S, Ikawa (2004) Brittle-ductile transition in monocrystalline silicon analysed by molecular dynamics simulation. P I Mech Eng C-J Mec 218(6):583–590
11. Arif M, Rahman M, San WY (2012) An experimental investigation into micro-ball end-milling of silicon. J Manuf Process 14(1): 52–61
12. Ohta T, Yan JW, Yajima S, Takahashi Y, Horikawa N, Kuriyagawa T (2007) High-efficiency machining of single-crystal germanium using large-radius diamond tools. Int J Surf Sci Eng 1(4):374–392

13. Goel S, Luo XC, Comley P (2013) Brittle-ductile transition during diamond turning of monocrystalline silicon carbide. Int J Mach Tool Manu 65(2):15–21
14. Arif M, Rahman M, San WY, Doshi N (2011) An experimental approach to study the capability of end-milling for microcutting of glass. Int J Adv Manuf Technol 53(9):1063–1073
15. Fang FZ, Hu H, Liu YC (2005) Modelling and experimental investigation on nanometric cutting of monocrystalline silicon. Int J Mach Tools Manuf 45(15):1681–1686
16. Liu Y, Li BZ, Wu CJ, Zheng YH (2016) Simulation-based evolution of surface micro-cracks and fracture toughness in high-speed grinding of silicon carbide ceramics. Int J Adv Manuf Technol 86(1):799–808
17. Huo DH, Lin C, Choong ZJ, Pancholi K, Degenaar P (2015) Surface and subsurface characterisation in micro-milling of monocrystalline silicon. Int J Adv Manuf Technol 81(5):1319–1331
18. Choong ZJ, Huo DH, Degenaar P, O'Neill A (2016) Effect of crystallographic orientation and employment of different cutting tools on micro-end-milling of monocrystalline silicon. P I Mech Eng B-J Eng 239(9):1756–1764
19. Rusnaldy TJK, Hee SK (2007) Micro-end-milling of single-crystal silicon. Int J Mach Tools Manuf 47(14):2111–2119
20. Rusnaldy TJK, Hee SK (2008) An experimental study on microcutting of silicon using a micromilling machine. Int J Adv Manuf Technol 39(1):85–91